Electronic Supplementary Information

Optimization of Photocarrier Dynamics and Activity in Phosphorene with Intrinsic Defects for Nitrogen Fixation

Wei Pei,[a] Si Zhou,[a,b*] Jijun Zhao,[a] Yi Du,[b] and Shi Xue Dou [b]

[a]*Key Laboratory of Materials Modification by Laser, Ion and Electron Beams (Dalian University of Technology), Ministry of Education, Dalian 116024, China*

[b]*Institute for Superconducting and Electronic Materials (ISEM), Australian Institute for Innovative Materials (AIIM), University of Wollongong, Wollongong, NSW 2500.*

[*] Corresponding author. E-mail: sizhou@dlut.edu.cn (Si Zhou)

S1. NAMD computational methods

To investigate the excited carrier dynamics in the defective black phosphorene (BP) and buckled blue phosphorene (BuP), NAMD simulations were carried out using the Hefei-NAMD codes.[1] We used velocity rescaling algorithm to remain the temperature of the system to around 300 K. After that, a 2 ps microcanonical *ab initio* MD trajectory was generated with a 1 fs time step. Only the Γ-point was used to sample the Brillouin zone. They are initial conditions for NAMD, which was obtained using fewest-switches surface hopping (FSSH) in the classical path approximation and with the decoherence correction.[2] The NAMD results were obtained by averaging over 50 different initial configurations radomly selected from the MD trajectory based on the classical path approximation.[3] In order to character the accuracy of our photogenrated carrier dynamics using PBE fuctional, we compared the electron density of states of defective phosphorene from PBE and HSE06 calculations. As shown in Fig. S1, the HSE06 functional increases the energy gap of the defective phosphorene with regard to PBE result, while the DOS shape exhibit good consistence between PBE and HSE06 functionals. Therefore, the PBE functional should be reasonable to describe the photoexcited charge dynamics in our work, considering the much higher computational cost using HSE06 functional.

To justify the accuracy of NAMD method, we examined the photocarrier dynamics in pristine BP monolayer. As shown in Figure S2 and Table S1 below, the BP monolayer exhibits slow *e–h* recombination with time scale of ~118 ps, which is well consistent with the experimental measurement (~100 ps).[4] According to the Fourier transform (FT) of band gaps, the nonradiative *e–h* recombination is dominated by the vibrational mode at ~400 cm^{-1} corresponding to the out-of-plane A_g^1 mode (experimental value at ~440 cm^{-1}).[4,5] The average fluctuation amplitude of band gap gives a fluorescence line width of 137 meV, close to the experimental value of 150 meV.[5] These evidences demonstrate that the NAMD method can predict reliable results on the photocarrier transport properties of phosphorene systems.

Table S1 The computational and experimental time scale (τ_{e-h}), vibration model (φ) and line with (ΔL) for prisitine BP monolayer electron–hole recombination.

	τ_{e-h} (ps)	φ (cm^{-1})	ΔL (meV)
Comput.	118	400	137
Exp.[4,5]	100	440	150

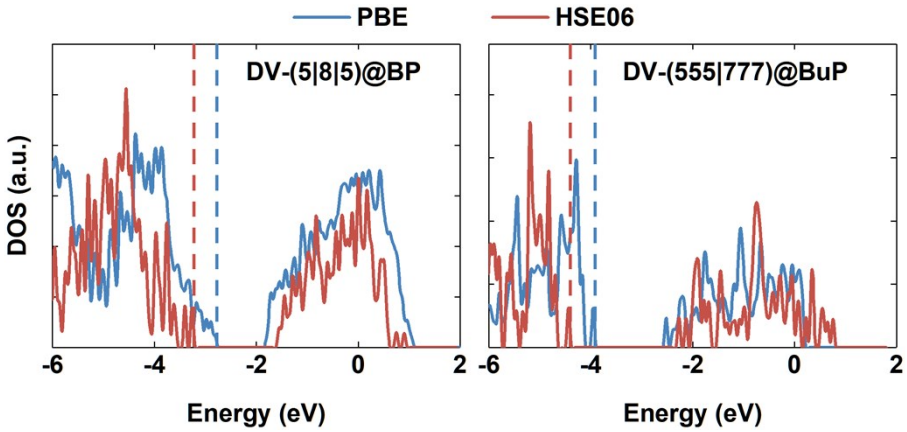

Fig. S1 Density of states of DV-(5|8|5)@BP (left panel) and DV-(555|777)@BuP (right panel) calculated using PBE and HSE06 functionals. The dashed color lines indicate the Fermi level. The vacuum energy is set as zero.

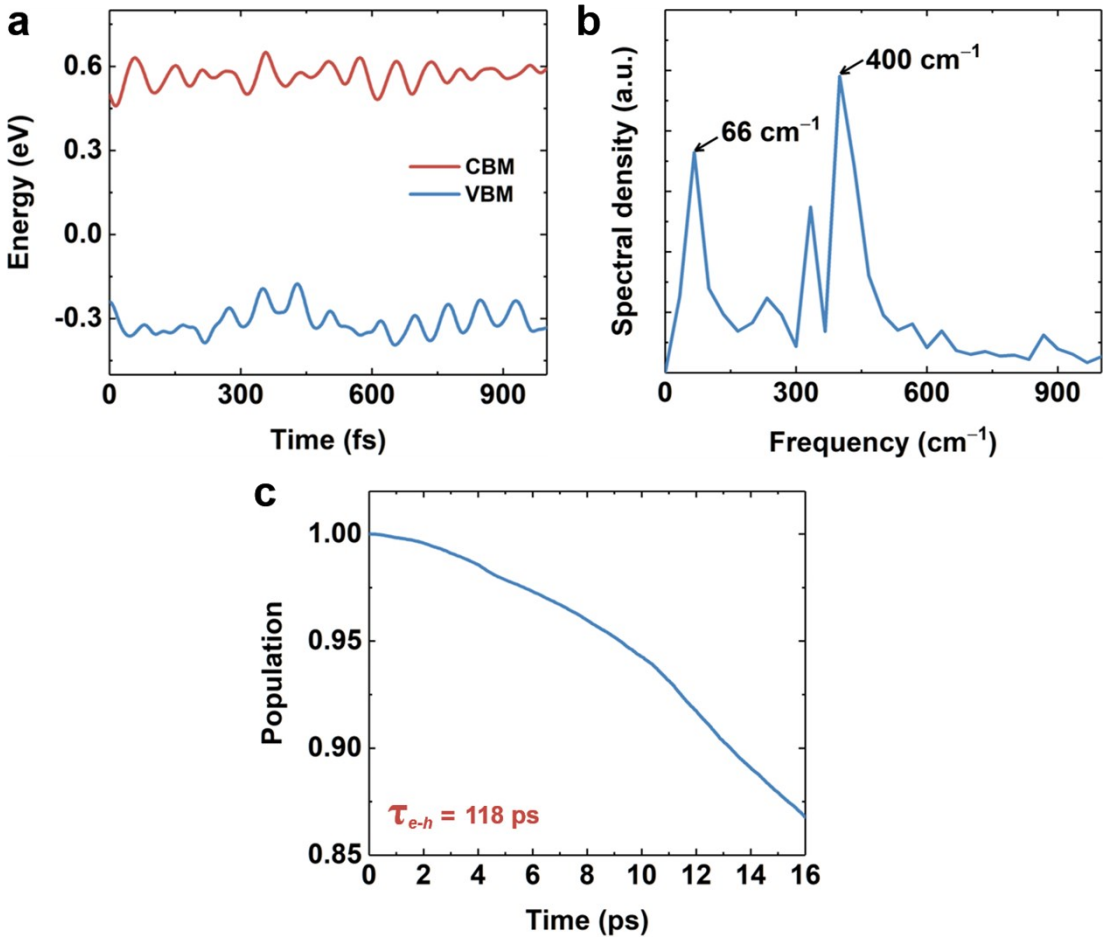

Fig. S2 (a) Time evolution of CBM and VBM orbital energies, (b) spectral density of band gap fluctuation, and (c) electron–hole recombination dynamics for pristine BP monolayer, respectively.

S2. Free energy calculation

Table S2 Zero-point energy (ZPE) and entropic correction (*TS*) at *T* =298.15 K for the molecules and intermediate species involved in N_2 reduction to NH_3. The ZPE and *TS* values of reaction intermediates adsorbed on SV-(5|9)@BP are presented and used throughout our calculations, which are close to the values for the other defective phosphorene systems.

Species	ZPE (eV)		*TS* (eV)		ZPE–*TS* (eV)	
	vacuum	solvation	vacuum	solvation	vacuum	solvation
*NN	0.17	0.38	0.29	0.09	–0.12	0.29
*N.*N	0.20	0.19	0.07	0.09	0.13	0.10
*N.*NH	0.50	0.51	0.07	0.09	0.43	0.42
*NH.*NH	0.82	0.81	0.08	0.10	0.74	0.71
N.NH_2	0.80	0.81	0.13	0.13	0.67	0.68
NH.NH_2	1.11	1.11	0.12	0.09	0.99	1.02
NH_2.NH_2	1.44	1.39	0.11	0.15	1.33	1.24
N.NH_3	1.10	1.15	0.12	0.18	0.98	0.97
NH.NH_3	1.40	1.37	0.21	0.30	1.19	1.07
*N	0.10	0.10	0.04	0.04	0.06	0.06
*NH	0.41	0.41	0.04	0.05	0.37	0.36
*NH_2.*NH3	1.70	1.68	0.28	0.29	1.42	1.39
*NH_2	0.72	0.71	0.06	0.09	0.66	0.62
*NH_3	0.96	0.98	0.07	0.22	0.89	0.76

S3. Reaction mechanism of NRR on defective BP and BuP

Table S3 Adsorption energies of nitrogen (ΔE_{*N2}) and ammonia molecule (ΔE_{*NH3}) and the limiting potentials for N_2 reduction to NH_3 (U_L) calculated in vacuum and using solvation model.

system	ΔE_{*N2} (eV)		ΔE_{*NH3} (eV)		U_L (V)	
	vacuum	solvation	vacuum	solvation	vacuum	solvation
SV-(5|9)@BP	1.30	1.09	–0.27	–0.35	–0.52	–0.32
DV-(5|8|5)@BP	1.26	1.26	–0.17	–0.10	–0.28	–0.29
DV-(4|10|4)@BP	0.25	0.26	0.48	0.44	–0.84	–0.37
DV-(555|777)@BP	1.64	1.46	0.12	0.21	–0.40	–0.37
SV@BuP	0.65	0.66	–0.68	–1.02	–0.29	–0.22
DV-(5|8|5)@BuP	1.73	1.48	–0.31	–0.18	–0.67	–1.00
DV-(555|777)@BuP	1.86	1.62	–0.09	–0.43	–0.34	–0.20

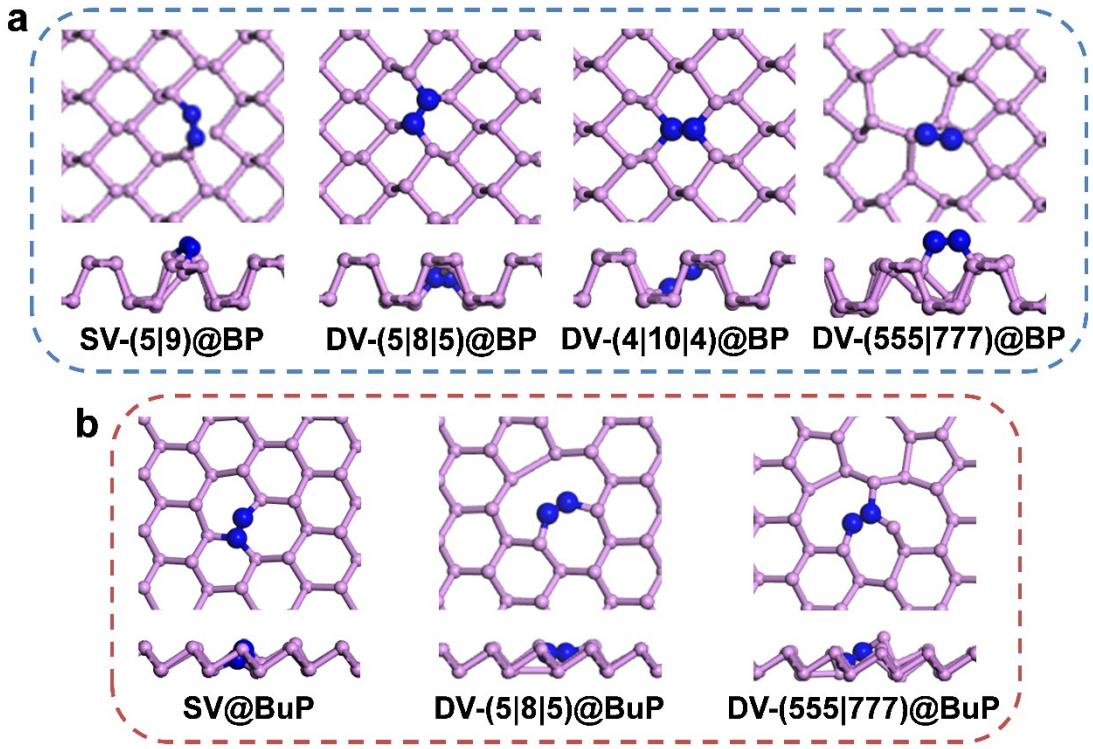

Fig. S3 Top and side views of N_2 adsorption on (a) defective black phosphorene, including single vacancy, namely, SV-(5|9)@BP, and double vacancies, namely, DV-(5|8|5)@BP, DV-(4|10|4)@BP and DV-(555|777)@BP (from left to right); (b) defected blue phosphorene monolayers including SV@BuP, DV-(5|8|5)@BuP and (555|777)@BuP. The N and P atoms are shown in blue and violet colors, respectively.

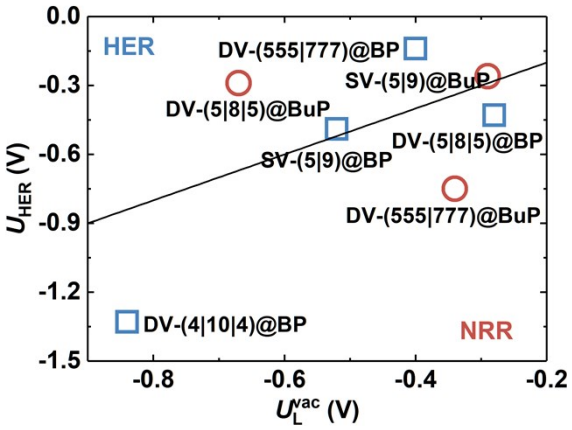

Fig. S4 The competition of limiting potentials between HER (U_{HER}) and NRR ($U_L{}^{vac}$) on various defective BP (blue squares) and BuP (red circles) systems. The black line indicates the boundary of chemical selectivity between HER and NRR.

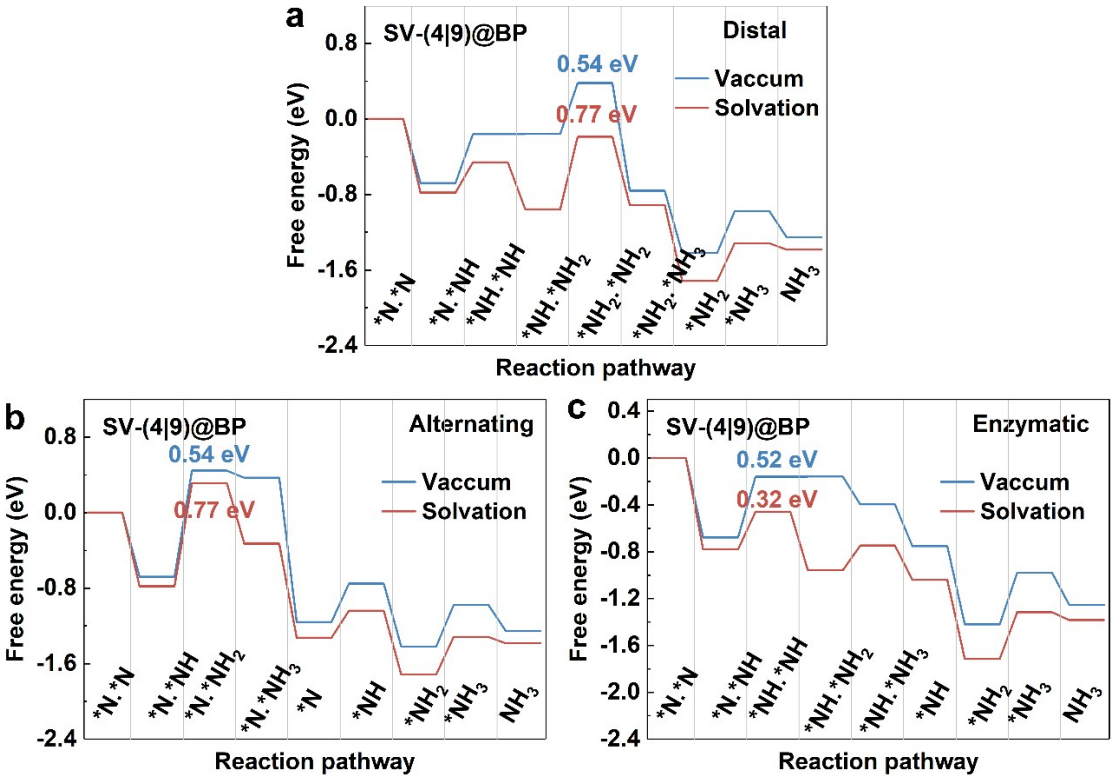

Fig. S5 Free energy diagrams of N_2 reduction to NH_3 on the SV-(4|9)@BP via (a) distal, (b) alternating and (c) enzymatic mechanisms calculated without (blue line) and with solvation effect (red line). The inset color numbers indicate the limiting step and the corresponding Gibbs free energy.

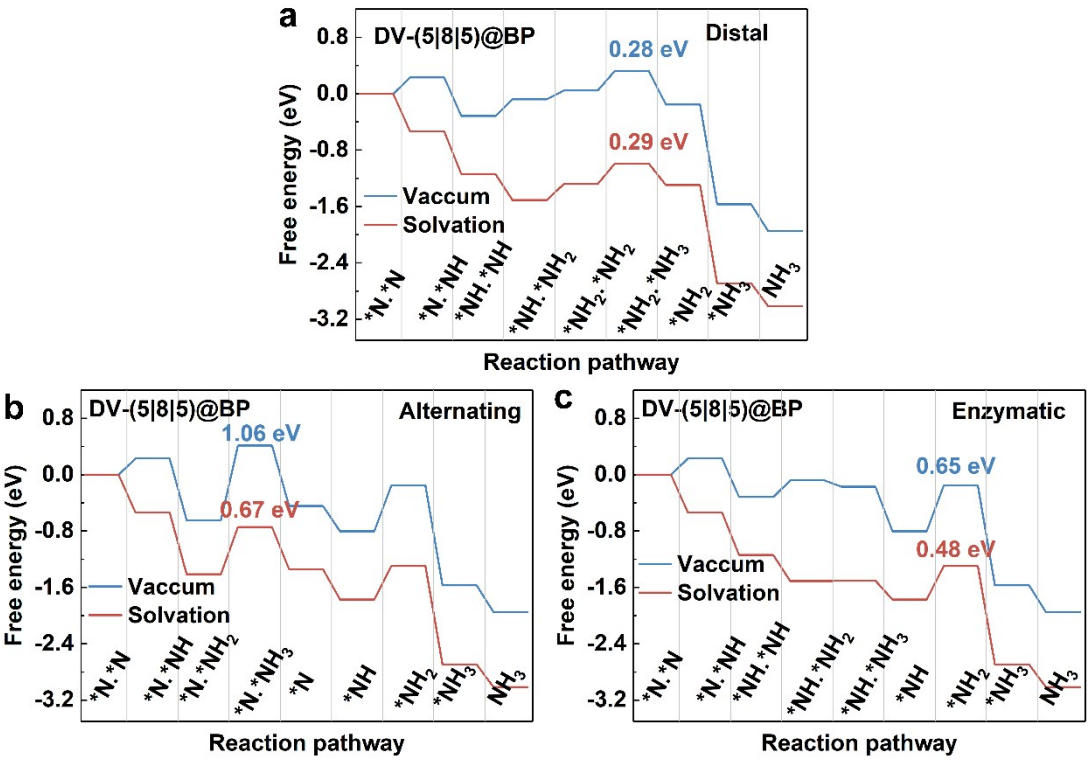

Fig. S6 Free energy diagrams of N_2 reduction to NH_3 on the DV-(5|8|5)@BP via (a) distal, (b) alternating and (c) enzymatic mechanisms calculated without (blue line) and with solvation effect (red line). The inset color numbers indicate the limiting step and the corresponding Gibbs free energy.

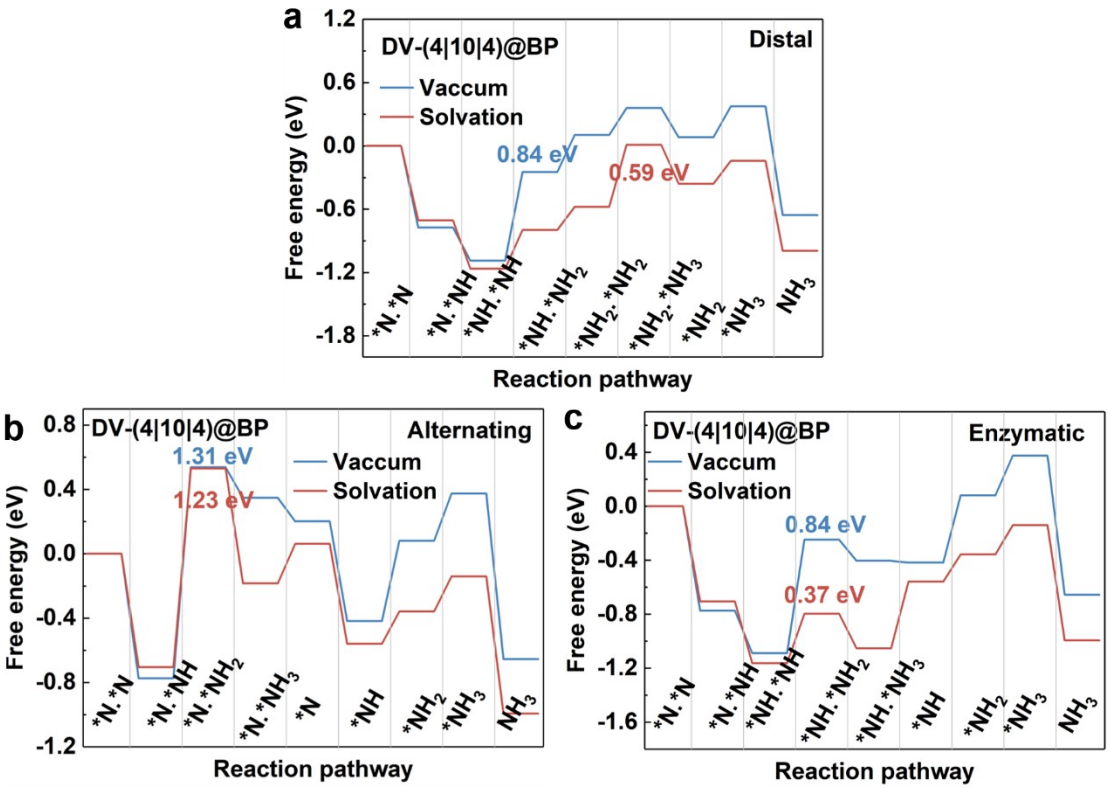

Fig. S7 Free energy diagrams of N_2 reduction to NH_3 on the DV-(4|10|4)@BP via (a) distal, (b) alternating and (c) enzymatic mechanisms calculated without (blue line) and with solvation effect (red line), respectively. The inset color numbers indicate the limiting step and corresponding Gibbs free energy.

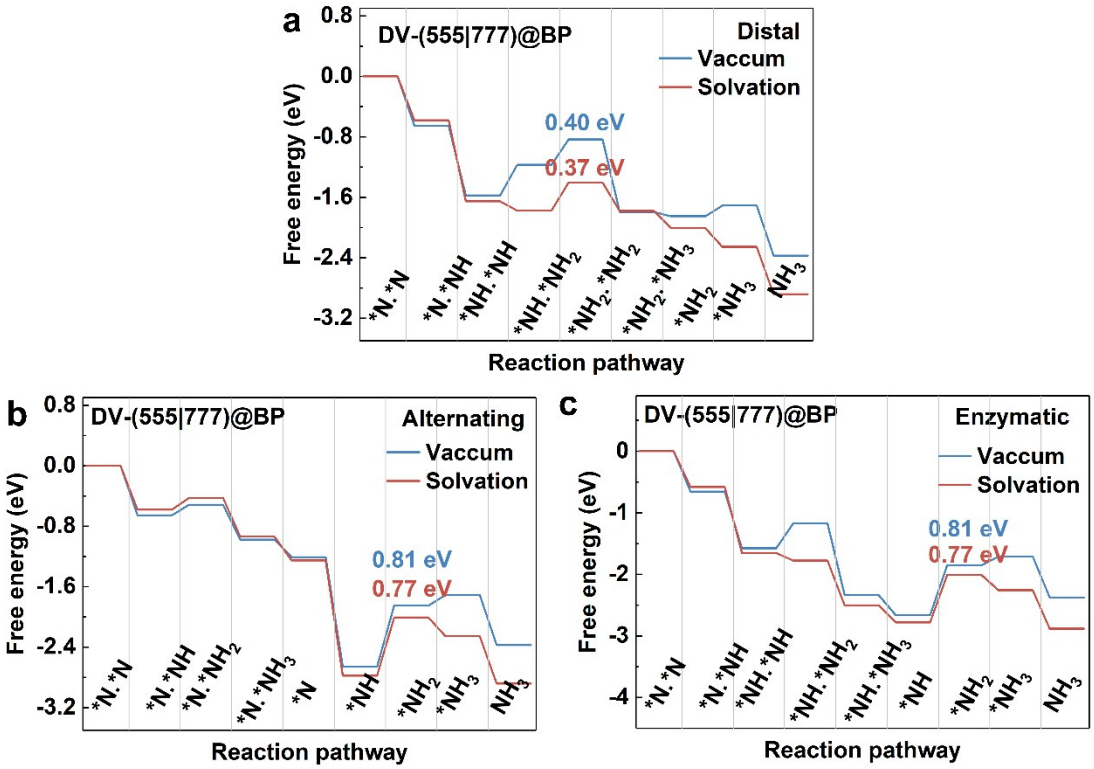

Fig. S8 Free energy diagrams of N_2 reduction to NH_3 on the DV-(555|777)@BP via (a) distal, (b) alternating and (c) enzymatic mechanisms calculated without (blue line) and with solvation effect (red line). The inset color numbers indicate the limiting step and the corresponding Gibbs free energy.

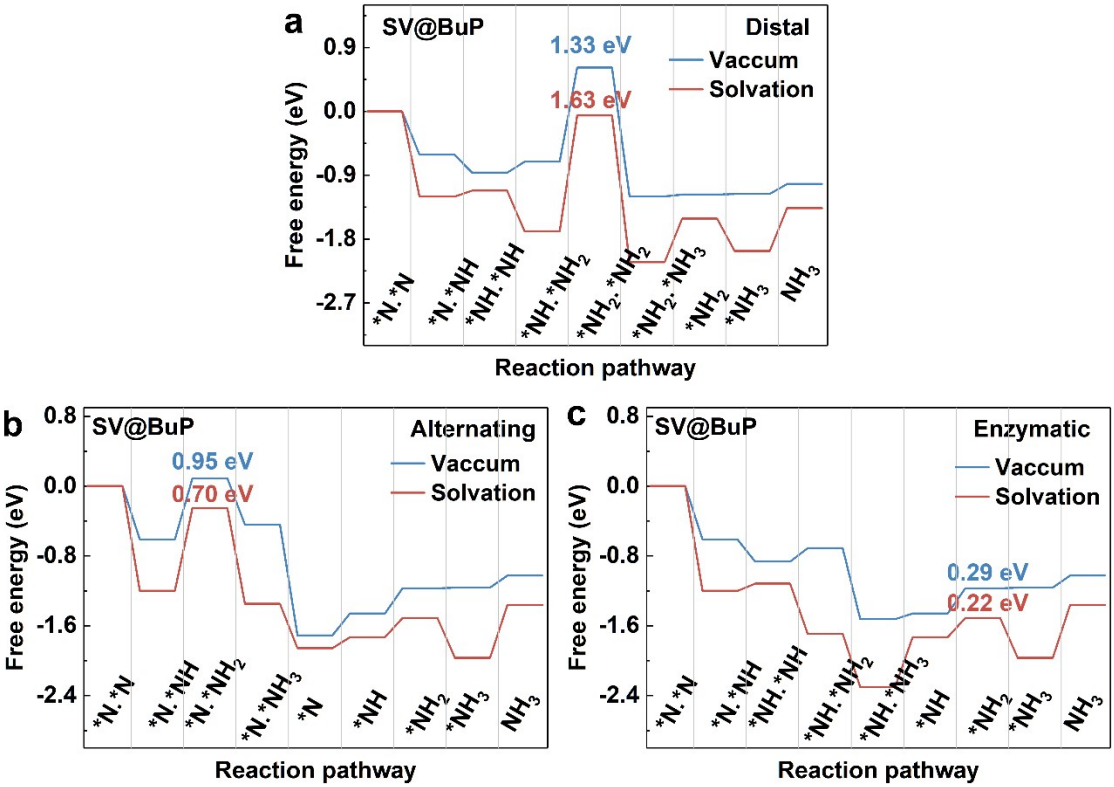

Fig. S9 Free energy diagrams of N_2 reduction to NH_3 on the SV@BuP via (a) distal, (b) alternating and (c) enzymatic mechanisms calculated without (blue line) and with solvation effect (red line). The inset color numbers indicate the limiting step and the corresponding Gibbs free energy.

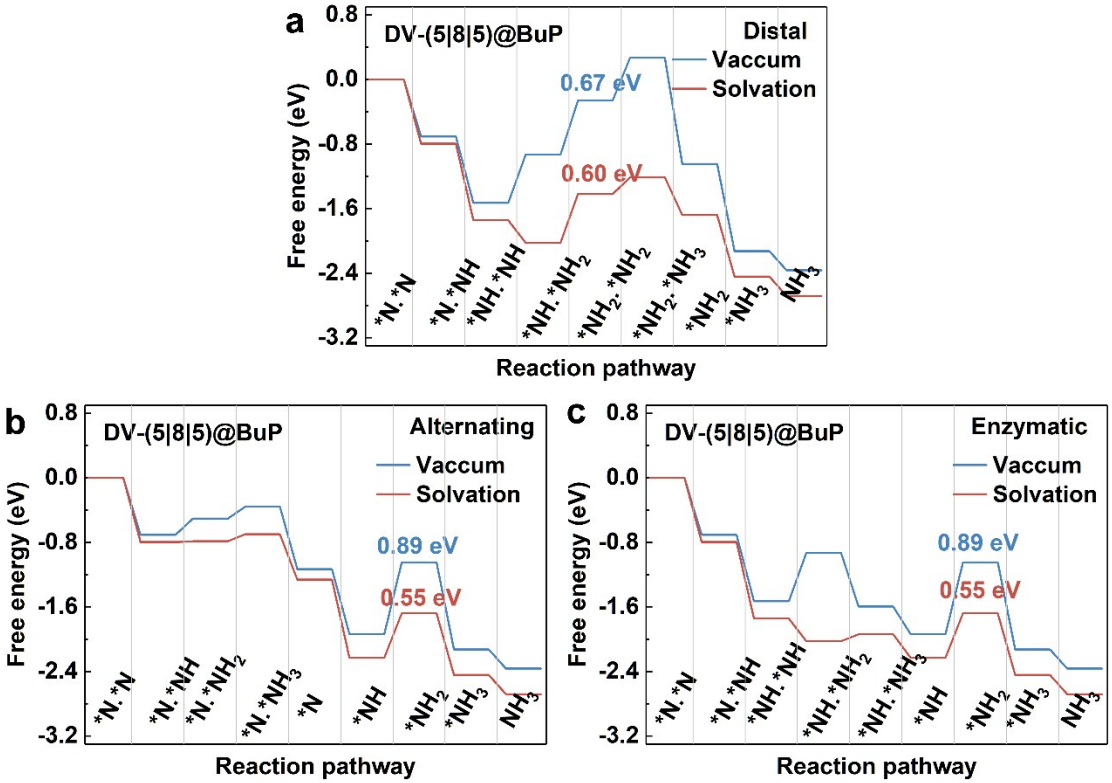

Fig. S10 Free energy diagrams of N_2 reduction to NH_3 on the DV-(5|8|5)@BuP via (a) distal, (b) alternating and (c) enzymatic mechanisms calculated without (blue line) and with solvation effect (red line). The inset color numbers indicate the limiting step and the corresponding Gibbs free energy.

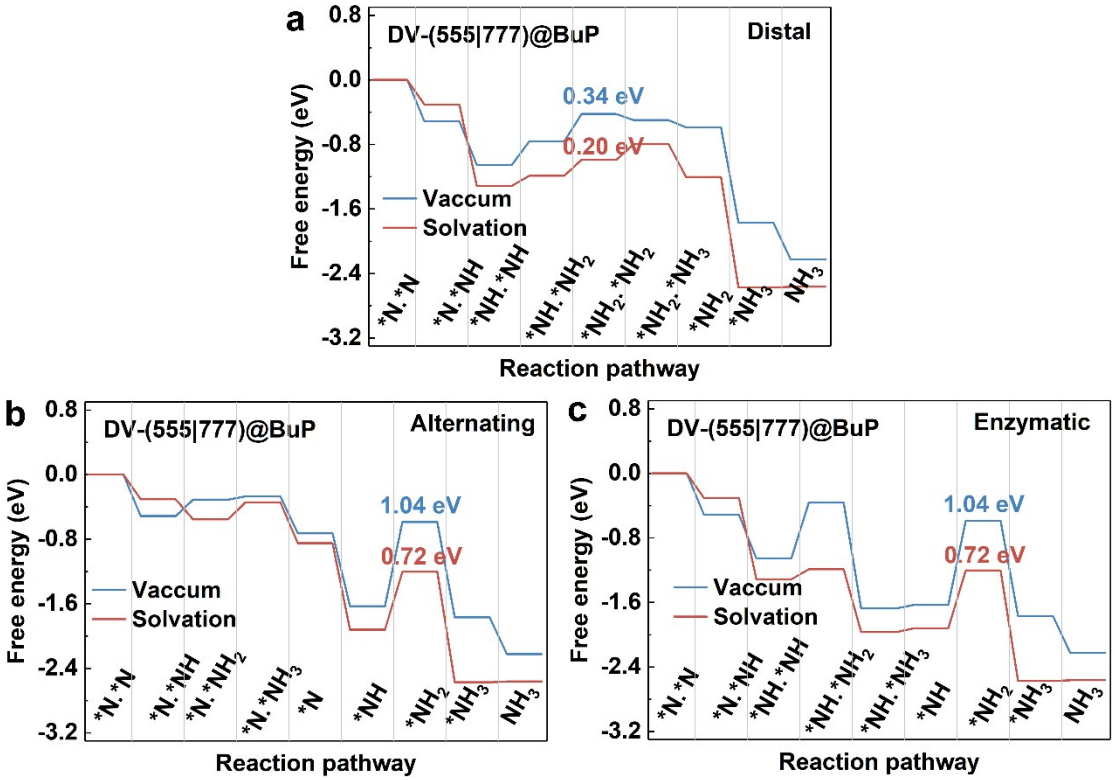

Fig. S11 Free energy diagrams of N_2 reduction to NH_3 on the DV-(555|777)@BuP via (a) distal, (b) alternating and (c) enzymatic mechanisms calculated without (blue line) and with solvation effect (red line). The inset color numbers indicate the limiting step and the corresponding Gibbs free energy.

S4. Electrinic structures of defected BP and BuP

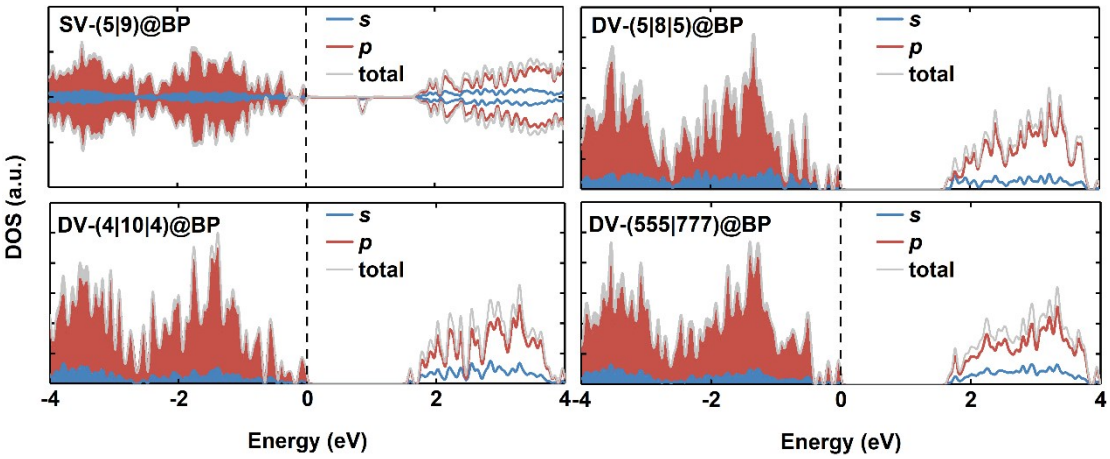

Fig. S12 The density of states (DOS) of various defective black phosphorene calculated by HSE06 functional. The colored solid lines and black dashed line indicate the orbital and Fermi level for each system, respectively. The occupied states are shadowed.

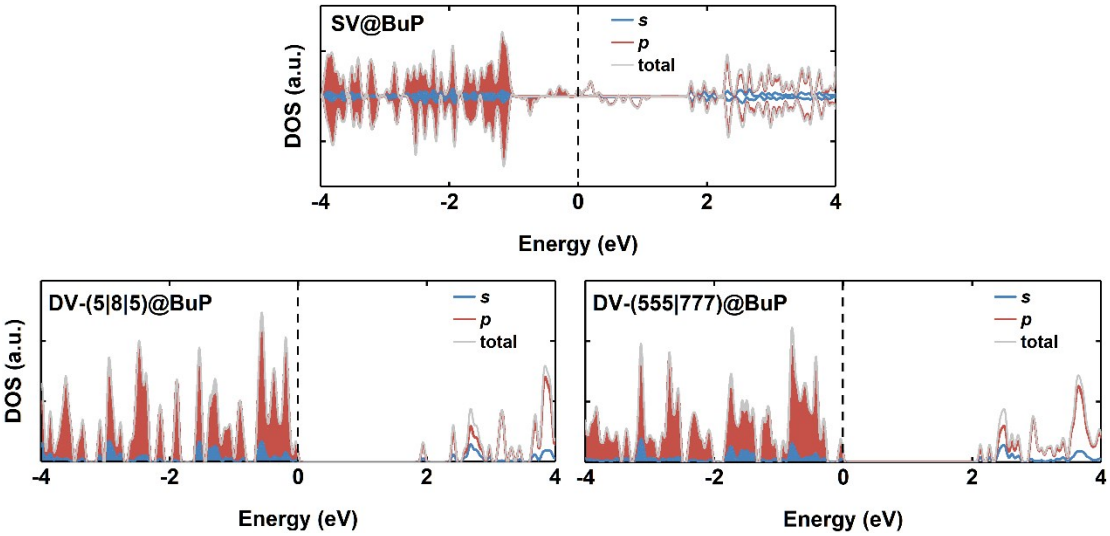

Fig. S13 The density of states (DOS) of various defective blue phosphorene calculated by HSE06 functional. The colored solid lines and black dashed line indicate the orbital and Fermi level for each system, respectively. The occupied states are shadowed.

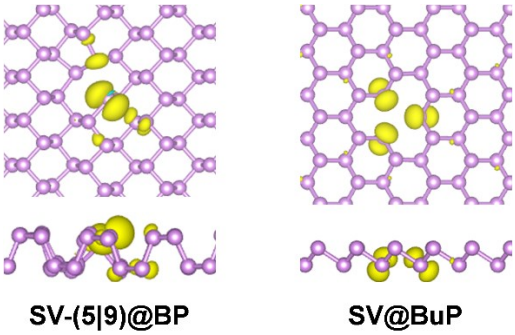

Fig. S14 Spin densities of BP (left) and BuP (right) with a SV defect. The isosurfacce value is 0.002 eÅ^{-3}

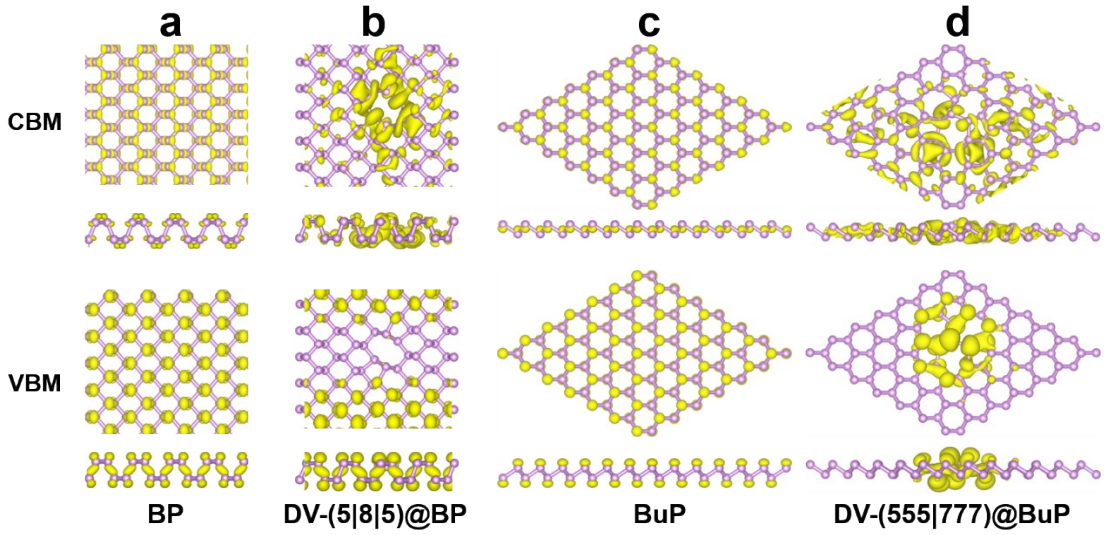

Fig. S15 Charge density of the CBM and VBMfor pristine (a) BP and (b) BuP, (c) DV-(5|8|5)@BP and (d) DV-(555|777)@BuP. The yellow color represents charge density with an isosurface value of 0.005 eÅ^{-3}.

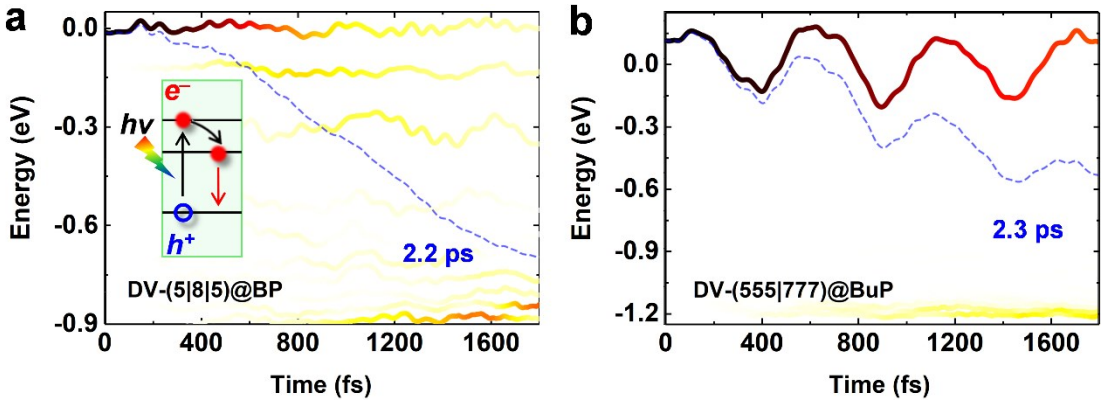

Fig. S16 The time-dependent averaged energy evolution (blue dashed lines) of electron-hole recombination (red arrow) for (a) DV-(5|8|5)@BP and (b) DV-(555|777)@BuP.

References

1 Q. Zheng, W. Chu, C. Zhao, L. Zhang, H. Guo, Y. Wang, X. Jiang and J. Zhao, *WIREs Comput. Mole. Sci.*, 2019, **9**, 1411–1437.

2 J. C. Tully, *J. Chem. Phys.*, 1990, **93**, 1061–1071.

3 B. J. Berne, *Classical and quantum dynamics in condensed phase simulations*, World Scientific, 1998.

4 J. He, D. He, Y. Wang, Q. Cui, M. Z. Bellus, H.-Y. Chiu and H. Zhao, *ACS Nano*, 2015, **9**, 6436–6442.

5 X.-B. Li, P. Gao, T.-F. Gao, H. Liu, W.-M, Lau and L.-M. Liu, Nat. Nanotechnol., 2015, **10**, 517–521.